Short Communication

A "soft table" for the natural frequencies and modal parameters of uniform circular plates with elastic edge support ☆

Andrei Zagrai*, Dimitri Donskoy

Davidson Laboratory, Stevens Institute of Technology, Hoboken, NJ 07030, USA

Abstract

The paper introduces a "soft table" for the natural frequencies and modal parameters of uniform circular plates with elastic edge support. In contrast to conventional tabulations on paper, the "soft table" allows to save space and display parameters for required number of vibration modes. The "soft table" is realized in a collection of Matlab® codes that calculate natural frequencies and mode shape parameters for a given set of translational and rotational constraints and modifiable Poisson ratio. Calculations of natural frequencies and modal parameters for a wide range of constraints revealed distinctive regions where the frequencies and parameters could change considerably. Knowing position and extension of these regions could be essential for design and vibration control of structures incorporating circular plates.
© 2005 Elsevier Ltd. All rights reserved.

1. Introduction

Continuous circular plates are widely used as structural elements in many aerospace, marine and civil applications. When subjected to the dynamic load, structures incorporating circular plates often exhibit several vibration modes, which may be associated with this structural element. As a result, vibrations of continuous uniform circular plates have been extensively studied for decades showing that straightforward and relatively simple analytical solutions exist for many complex problems. Recent investigations have reiterated the efficiency of the classical approach [1,2] in analyzing the dynamic behavior of variety of structures ranging from a riveted hatch [3] and viscoelastic sandwich circular plate [4] to applications in damage detection [5] and smart materials [6].

Although the circular symmetry of the problem allows for its significant simplification, additional difficulties often arise due to uncertainty of boundary conditions. This uncertainty occurs because, in many practical applications, the edge of the plate is not free, clamped, or simply-supported. When the plate's boundary conditions depart from "classical" cases, elastic translational and rotational constraints should be considered. One of the earliest formulations of this problem was presented by Leissa [1], who tabulated a frequency parameter for four vibration modes of a simply supported circular plate with varying rotational stiffness. Further extension of the work [7] included numerical results obtained using the Fourier solution and the Ritz method. Avalos et al. [8,9] studied vibrations of stepped circular plates elastically restrained against both translation and rotation. Authors presented an approximate solution in terms of polynomial coordinate functions and tabulated results for a number of vibration modes. Tabulations provided by Avalos et al. are perhaps the most comprehensive reference available on the subject. It should be noted, however, that only four values of translational and rotational stiffnesses were considered (two of which are 0 and ∞) and a very limited number of vibration modes were presented. Azimi [10] reported a broader range of results for both edge and interior supports, but rotational constraints were not included in the study. The effect of internal elastic translational supports was recently investigated by Wang and Wang [11], who observed the switching between axisymmetric and asymmetric vibration modes. An extensive review of the modal properties of the elastically restrained beams and plates was presented by Kang and Kim [12]. Authors followed the analytic approach in calculating the complex rotational and translational stiffnesses and a complex loss factor. The results for the first vibration mode of the circular plate were shown as a 3-D dependence of a normalized natural frequency and loss factor versus rotational and translational stiffnesses. Unfortunately, the authors did not tabulate their results. In contrast, Ashour [13], who studied vibration of variable thickness elastically restrained rectangular plates, presented illustrations for two vibration modes and tabulated frequency parameters up to the fifth mode.

It is worth noting that circular plates are widely used in modeling various fluid–structure interaction problems. Previous assumptions of the "classical" boundary conditions (for example free plate in Ref. [14]) were recently expanded by Rdzanek et al. [15], who included effects of rotational and translational edge stiffnesses in the analytical formulae for the radiated sound power.

The literature shows that although vibration of elastically restrained circular plates is of a considerable interest, availability of tabulated data is severely limited. In particular, previous

studies that considered circular plates with both translational and rotational constraints were restricted to a few low-frequency vibration modes. For these modes, the frequency parameter was calculated using only several translational and rotational stiffnesses in a $0-\infty$ range (4 in Ref. [8,9] and 2 in Ref. [15]). Thus, it is very difficult to use these results in establishing potential data trends. In contrast to studies on the free edge plates [14,16], no data are available for a mode shape parameter and on the effect of the Poisson ratio.

The purpose of this paper is to provide an extensive "soft" reference table that: (a) considers a general case of an elastic boundary condition at the plate's circumference, i.e. both translational and rotational constraints; (b) includes frequency and mode shape parameters; (c) permits tabulating parameters for various Poisson coefficients; (d) allows for representing a desired number of mode shapes; (e) could be incorporated as a subroutine in other research codes.

2. Analytical formulation

In the classical plate theory [1,2], the following fourth-order differential equation describes free flexural vibrations of a thin circular uniform plate:

$$D \cdot \nabla^4 w(r, \theta, t) + \rho h \partial^2 w(r, \theta, t)/\partial t^2 = 0 \tag{1}$$

where $D = Eh^3/12(1-v^2)$ is the flexural rigidity of a plate and h, ρ, E, v are the plate's thickness, density, Young's modulus and the Poisson ratio, respectively. Displacement in Eq. (1) can be presented as a combination of spatial and time-dependent components $w(r, \theta, t) = W(r, \theta)T(t)$. It is well established that the spatial solutions of Eq. (1) are flexural mode shapes of the form

$$W_{mn}(r, \theta) = A_{mn}(J_n(\Lambda_{mn}r/a) + C_{mn}I_n(\Lambda_{mn}r/a))\cos(n\theta), \quad n > 0, \tag{2}$$

where a is a radius of the plate and Λ_{mn}, C_{mn}, A_{mn} are the eigenvalues, mode shape parameters and normalization constants. Indexes m and n are positive integers and correspond to the number of concentric circles and nodal diameters in each flexural mode. It is apparent from Eq. (2) that in order to describe a flexural mode we need to know Λ_{mn}, C_{mn}, A_{mn}. These constants are determined from boundary and normalization conditions.

Considering an elastically supported plate presented in Fig. 1, boundary conditions (at $r = a$) can be formulated in terms of effective translational K_T and rotational K_R stiffnesses

$$M_r(a, \theta) = K_R \frac{\partial W}{\partial r}(a, \theta), \tag{3}$$

and

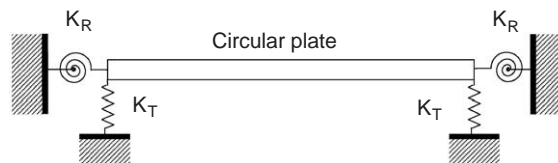$$V_r(a, \theta) = -K_T W(a, \theta), \tag{4}$$

Fig. 1. A thin circular plate with translational K_T and rotational K_R elastic edge constraints.

where the bending moment and the Kelvin–Kirchhoff shearing force are defined as

$$M_r = -D\left[\frac{\partial^2 W}{\partial r^2} + v\left(\frac{1}{r}\frac{\partial W}{\partial r} + \frac{1}{r^2}\frac{\partial^2 W}{\partial \theta^2}\right)\right] \tag{5}$$

and

$$V_r = -D\left[\frac{\partial}{\partial r}\nabla^2 W + (1-v)\frac{1}{r}\frac{\partial}{\partial \theta}\left(\frac{1}{r}\frac{\partial^2 W}{\partial r\partial \theta} - \frac{1}{r^2}\frac{\partial W}{\partial \theta}\right)\right]. \tag{6}$$

Combining Eqs. (3)–(5) and (4)–(6) we obtain two equations for mode shape parameter C_{mn}:

$$C_{mn} = -\frac{Jp2 - \frac{2}{\Lambda_{mn}}\left(v + \frac{aK_R}{D}\right)Jm1 - \left(2 + \frac{4vn^2}{\Lambda_{mn}^2}\right)J_n(\Lambda_{mn})}{Ip2 + \frac{2}{\Lambda_{mn}}\left(v + \frac{aK_R}{D}\right)Ip1 + \left(2 - \frac{4vn^2}{\Lambda_{mn}^2}\right)I_n(\Lambda_{mn})} \tag{7}$$

and

$$C_{mn} = -\frac{-Jm3 + \frac{2Jp2}{\Lambda_{mn}} + \left(3 + \frac{4+4(2-v)n^2}{\Lambda_{mn}^2}\right)Jm1 + \left(\frac{8(3-v)n^2}{\Lambda_{mn}^3} - \frac{4}{\Lambda_{mn}} - \frac{8a^2K_T}{\Lambda_{mn}^3 D}\right)J_n(\Lambda_{mn})}{Ip3 + \frac{2Ip2}{\Lambda_{mn}} + \left(3 - \frac{4-4(2-v)n^2}{\Lambda_{mn}^2}\right)Ip1 + \left(\frac{8(3-v)n^2}{\Lambda_{mn}^3} + \frac{4}{\Lambda_{mn}} - \frac{8a^2K_T}{\Lambda_{mn}^3 D}\right)I_n(\Lambda_{mn})}, \tag{8}$$

where

$$Jm1 = J_{n+1}(\Lambda_{mn}) - J_{n-1}(\Lambda_{mn}), \quad Jp2 = J_{n+2}(\Lambda_{mn}) + J_{n-2}(\Lambda_{mn}),$$
$$Jm3 = J_{n+3}(\Lambda_{mn}) - J_{n-3}(\Lambda_{mn}), \quad Ip1 = I_{n+1}(\Lambda_{mn}) + I_{n-1}(\Lambda_{mn}),$$
$$Ip2 = I_{n+2}(\Lambda_{mn}) + I_{n-2}(\Lambda_{mn}), \quad Ip3 = I_{n+3}(\Lambda_{mn}) + I_{n-3}(\Lambda_{mn}).$$

Elimination of C_{mn} between Eqs. (7) and (8) yields the frequency equation, which allows to determine eigenvalues Λ_{mn}. For these eigenvalues, the mode shape parameters C_{mn} could be calculated using Eq. (7) or Eq. (8).

The amplitude of each vibration mode in Eq. (2) is set by the normalization constant A_{mn} calculated according to the following normalization condition:

$$\int_0^{2\pi}\int_0^a W_{mn}(r,\theta)W_{pq}(r,\theta)r\,dr\,d\theta = M\delta_{mp}\delta_{nq}, \tag{9}$$

where M is a mass of the plate; $\delta_{mp} = \delta_{nq} = 1$ if $m = p$, $n = q$ and $\delta_{mp}\delta_{nq} = 0$ if $m \neq p$ or $n \neq q$.

Considering mode shapes (2) in the normalization condition (9), the dimensionless normalization constant A_{mn} is

$$A_{mn} = \left[\frac{1}{\pi a^2}\int_0^{2\pi}\int_0^a ((J_n(\Lambda_{mn}r/a) + C_{mn}I_n(\Lambda_{mn}r/a))\cos(n\theta))^2 r\,dr\,d\theta\right]^{-1}. \tag{10}$$

In Eqs. (2) and (3), $\omega_{mn} = (\Lambda_{mn}^2/a^2)\sqrt{D/\rho h}$ is a natural frequency of flexural vibrations dependent on the eigenvalues Λ_{mn} and plate's radius a.
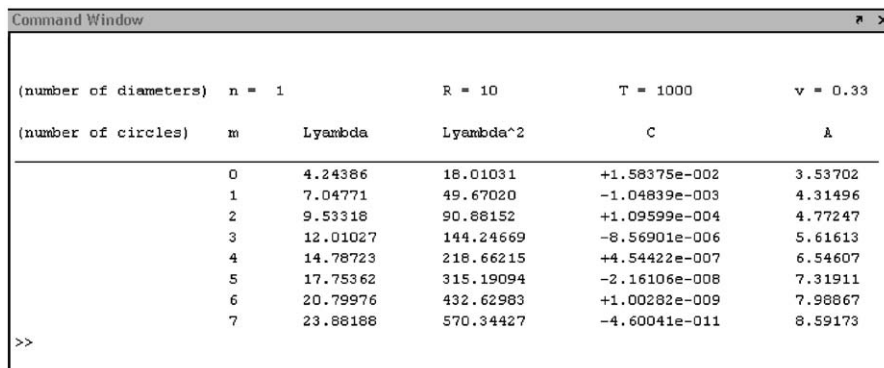
3. Matlab® code

Eqs. (7)–(10) were implemented in the Matlab® code `CP_elastic.m` which calculates eigenvalues Λ_{mn}, modal parameters C_{mn} and normalization constants A_{mn} for a given set of elastic boundary conditions. These boundary conditions were defined as follows:

$$\text{T} = a^3 K_T/D, \quad \text{R} = aK_R/D. \tag{11,12}$$

The input parameters of the program include: transverse and rotational stiffness ratios (11) and (12), Poisson ratio v, `N`—upper bond for eigenvalues Λ_{mn}, suggested step for Λ_{mn} finding$-$`d`, and a number of mode shape diameters$-$`n`. For a given input parameters, `CP_elastic.m` calculates Λ_{mn} on the interval [`0 d*N`] using a build in Matlab® root finding function `fzero`. This is achieved via subroutine `elastic_flexural.m` containing Eqs. (7) and (8). The algorithm first attempts to find zeros of Eqs. (7) and (8) on the interval [`0 d`]. Then, it records results of the search, progresses to the next interval `d`, and continues root finding until `d*N` is reached. Essentially, this procedure defines a vector of m eigenvalues Λ_m for a given n. Calculated eigenvalues are then used in `elastic_flexural_C.m` subroutine (Eq. (7)) to obtain C_m. An integral expression (10) gives normalization constants A_m. The code `CP_elastic.m` allows for displaying calculated parameters in a desired format and saving data using Matlab's "`diary on`" feature. The output window of the code with calculated modal parameters is shown in Fig. 2. Due to the open architecture of the program, a user can modify both the algorithm for calculating modal parameters and representation/saving of the data. To run the code, one needs to copy `CP_elastic` folder into Matlab's `work` directory and open `CP_elastic.m`.

4. Results and discussion

The advantage of the developed code is that it provides a reference for any translational and rotational constraints including intermediate values. The Poisson ratio could be adjusted accounting to various materials of the plate. Such a broad range of results, to our knowledge, is not available in the literature yet. However, we have compared the obtained results with


```
Command Window                                                        ↗ ✕

(number of diameters)   n =  1              R = 10          T = 1000      v = 0.33

(number of circles)     m      Lyambda     Lyambda^2          C              A

                        0      4.24386     18.01031      +1.58375e-002     3.53702
                        1      7.04771     49.67020      -1.04839e-003     4.31496
                        2      9.53318     90.88152      +1.09599e-004     4.77247
                        3     12.01027    144.24669      -8.56901e-006     5.61613
                        4     14.78723    218.66215      +4.54422e-007     6.54607
                        5     17.75362    315.19094      -2.16106e-008     7.31911
                        6     20.79976    432.62983      +1.00282e-009     7.98867
                        7     23.88188    570.34427      -4.60041e-011     8.59173
>>
```

Fig. 2. Output of the program showing calculated eigenvalues and modal parameters for a particular set of R, T and Poisson ratio v.

previously published data. The illustration of one of such comparisons is presented in Table 1, depicting eigenvalues, mode shape parameters and normalization constants for the first vibration mode. For the squared eigenvalues, i.e. $\Omega_{mn} = \Lambda_{mn}^2$, the agreement with previous works is 0.07% [8] and 0.14% [10]. The precision of the results in most of the references is three significant digits. Our calculations were done to 12 significant digits and the values averaged to 4 significant digits are presented in Table 1. Precision of results was controlled by the Matlab® algorithm for calculating Bessel functions.

Due to space limitation, we do not present comparison for higher vibration modes, but they are in good agreement, which can be easily verified by a reader. Table 1 does not include any comparison of mode shape parameter C_{mn} and normalization constants A_{mn} because, for the case of the elastic support, we did not find any published data. Refs. [14,16], which include data for C_{mn}, consider plates with free edge. The A_{mn} is tabulated by Itao and Crandall [16]. The results obtained with the developed code are in very good agreement with these two references.

Fig. 2 shows that the program determines modal parameters for a specific set of boundary conditions and Poisson ratio. However, core elements of the code could be included in other algorithmic structures for automation of laborious calculations or establishing potential data trends. This approach was used to obtain dependencies for Λ_{mn} depicted in Fig. 3. In the figure, we present eigenvalues Λ_{mn} as a function of translational (T) and rotational (R) constraints that varied in the 10^{-2}–10^6 range.

Small R and T (i.e. when both $R \to 0$ and $T \to 0$) in the figure exemplify the "free edge" boundary condition while large R and T ($R \to \infty$ and $T \to \infty$) correspond to the "clamped"

Table 1
Frequency and mode shape parameters for the mode 00; Poisson ratio is 0.3

|		Pr.	[8,10]	Pr.	—	Pr.	[8,10]	Pr.	[10]	Pr.	[8,10]
R	T:		0	10^{-2}		1		10^2		∞	
∞	Ω_{00}	—	—	0.1414	1.4068	1.406	8.8232		10.216	10.215
	C_{00}	—	—	0.9652	0.7031		0.0909		0.0557	
	A_{00}	—	—	0.5089	0.5993		1.8460		2.2152	
10^2	Ω_{00}	—	—	0.1414	1.4064		8.6878		10.019	
	C_{00}	—	—	0.9645	0.6982		0.0898		0.0557	
	A_{00}	—	—	0.5091	0.6014		1.8399		2.1942	
1	Ω_{00}	—	—	0.1414	1.3880	1.387	5.6964		6.0629	6.062
	C_{00}	—	—	0.9360	0.5190		0.0228		0.0092	
	A_{00}	—	—	0.5168	0.6892		1.8072		1.9279	
10^{-2}	Ω_{00}	—	—	0.1414	1.3740		4.7416		4.9499	
	C_{00}	—	—	0.9145	0.4096		−0.0272		−0.0361	
	A_{00}	—	—	0.5227	0.7560		1.8631		1.9440	
0	Ω_{00}	—	—	0.1414	1.3737	1.374	4.7287	4.735	4.9352	4.942
	C_{00}	—	—	0.9142	0.4078	1.373	−0.0281		−0.0369	4.935
	A_{00}	—	—	0.5228	0.7572		1.8643		1.9446	
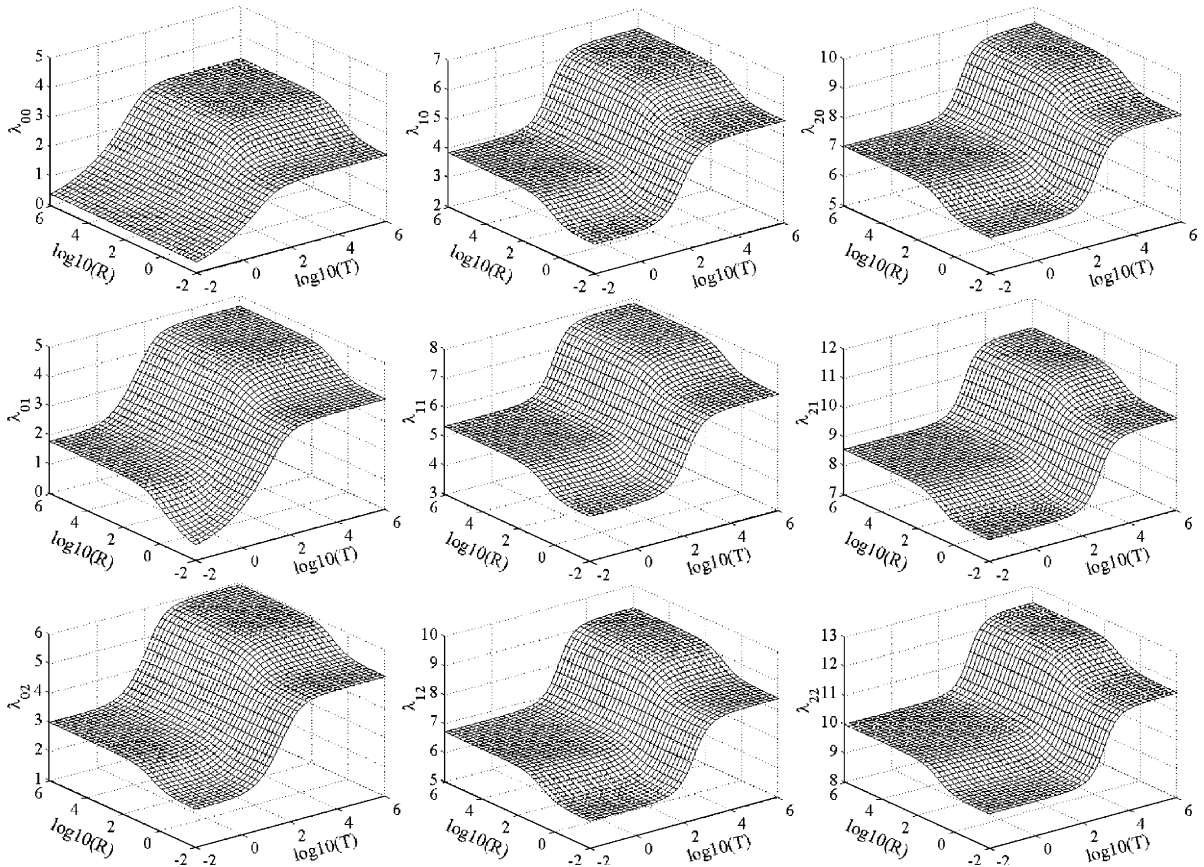
Fig. 3. Eigenvalues λ_{mn} calculated for the range of translational and rotational constraints.

case. The "simply supported" boundary conditions could be accounted for by setting $R \to 0$ and $T \to \infty$. Fig. 3 shows that the distribution of eigenvalues is not uniform and its shape significantly depends on vibration mode. For example, when $T \to 0$ the eigenvalues Λ_{00} of the first vibration mode approach zero because the plate exhibits rigid body translation. This translation is unaffected by rotational constraints, whose contribution is noticeable only at large T. However, a distinctively different situation is observed for the Λ_{01} vibration mode with one nodal diameter that features smooth transition from the rigid body rocking at $R \to 0$ and $T \to 0$ to vibrations controlled by rotational constraints at arbitrary R and $T \to 0$. In contrast to the rigid body translation, rocking could be restrained by rotational constraints. Fig. 3 shows several regions where eigenvalues Λ_{mn} change noticeably. The smoothened stepped variation is observed for both R and T and the steepness increases with the mode number. As the mode number increases, the stepped region moves toward the "clamped" boundary condition. Interestingly, stepped variation of T is much more profound than that of the R. For instance, for nine vibration modes presented in Fig. 3, position of the stepped region with respect to R changed very little and falls within 1–100 range. In contrast, position of the stepped region with respect to T moved gradually from the

Table 2
Frequency parameter Ω_{10} calculated for various Poisson ratios and respective translational (T) and rotational (R) constraints

T, R	Poisson ratio						
	0.1	0.2	0.3	0.4	0.5	0.6	0.7
$T = 0$, $R = 0$	8.51982	8.77183	9.00314	9.21637	9.41367	9.59685	9.76745
$T = 1$, $R = 1000$	14.73613	14.73613	14.73613	14.73613	14.73613	14.73613	14.73613
$T = 100$, $R = 100$	22.14098	22.14098	22.14099	22.14099	22.14099	22.14099	22.14099
$T = 1000$, $R = 1$	29.59984	29.67881	29.75614	29.83191	29.90614	29.97888	30.05017
$T = 10^{12}$, $R = 10^{12}$	39.77115	39.77115	39.77115	39.77115	39.77115	39.77115	39.77115

range of 1–100 to 10^2–10^4. Knowing position of the region where eigenvalues change drastically is essential for vibration control and structural design.

Table 2 shows the effect of Poisson ratio on the frequency parameter Ω_{10} for various boundary conditions around the plate's circumference. An analytical solution for the "clamped" case is known to be independent on Poisson ratio v [1]. Similarly, numerical calculations for $R \to \infty$ and $T \to \infty$ show that Ω_{10} is unaffected by v. In contrast to the "clamped" boundary condition, Ω_{10} for the "free" plate increases considerably with increase in Poisson ratio. This observation is consistent with the results obtained in Ref. [14] for "free" plates. Table 2 illustrates that for small R results are dependent on v. If R is large, frequency parameter Ω_{10} are v independent for any T.

5. Conclusions

This paper introduced a "soft table" for eigenvalues, mode shape parameters and normalization coefficients of a circular plate with elastic (translational and rotational) edge supports. The "soft table" is realized in an open Matlab® code [17] and is available for free download from the file exchange website (http://www.mathworks.com/matlabcentral/fileexchange/) or from one of the author's website (http://personal.stevens.edu/~azagrai/index/publications.html). In contrast to conventional approach which represents calculated results in a tabular format on paper, the "soft table" allows to save space and display virtually any number of modal parameters. The program could be conveniently modified by a user and advantageously used either as a reference tool or as a subroutine in related research projects.

Comparison of results presented in this paper with the results of previously published research shows good agreement. Three-dimensional plots of eigenvalues and mode shape parameters versus wide range of translational and rotational constraints could be potentially used in structural design and vibration control. For instance, Fig. 3 shows that eigenvalues change drastically only in a limited range of constraints specific to each vibration mode and are stable elsewhere. Effect of the Poisson ratio is considerable only for the "free" plate but could be still noticeable for weak rotational constraints. The "soft table" code allows for duplicating this work and further expanding presented results to include higher vibration modes or other Poisson ratios.

Acknowledgements

References

[1] A.W. Leissa, *Vibration of Plates*, SP-160, NASA, US Government Printing Office, Washington, DC, 1969.

[2] W. Soedel, *Vibrations of Shells and Plates*, Marcel Dekker, New York, 1993.

[3] M. Amabili, R. Pierandrei, Analysis of vibrating circular plates having non-uniform constraints using the modal properties of free-edge plates: application to bolted plates, *Journal of Sound and Vibration* 206 (1) (1997) 23–38.

[4] S.-C. Yu, S.-C. Huang, Vibration of a three-layered viscoelastic sandwich circular plate, *International Journal of Mechanical Sciences* 43 (2001) 2215–2236.

[5] P.F. Pai, Y. Oh, S.-Y. Lee, Detection of defects in circular plates using a scanning laser vibrometer, *International Journal of Structural Health Monitoring* 1 (1) (2002) 63–88.

[6] A.N. Zagrai, V. Giurgiutiu, Electro-mechanical impedance method for crack detection in thin plates, *Journal of Intelligent Material Systems and Structures* 12 (10) (2001) 709–718.

[7] A.W. Leissa, P.A.A. Laura, R.H. Gutierrez, Transverse vibrations of circular plates having nonuniform edge constraints, *Journal of the Acoustical Society of America* 66 (1) (1979) 180–184.

[8] D. Avalos, P.A.A. Laura, A.M. Bianchi, Analytical and experimental investigation on vibrating circular plate with stepped thickness over a concentric circular region, *Journal of the Acoustical Society of America* 82 (1) (1987) 13–16.

[9] D. Avalos, P.A.A. Laura, H.A. Larrondo, Vibrating circular plates with stepped thickness over a concentric circular region: a general, approximate solution, *Journal of the Acoustical Society of America* 84 (4) (1988) 1181–1185.

[10] S. Azimi, Free vibration of circular plates with elastic or rigid interior support, *Journal of Sound and Vibration* 120 (1) (1988) 37–52.

[11] C.Y. Wang, C.M. Wang, Fundamental frequencies of circular plates with internal elastic ring support, *Journal of Sound and Vibration* 263 (2003) 1071–1078.

[12] K.-H. Kang, K.-J. Kim, Modal properties of beams and plates on resilient supports with rotational and translational complex stiffness, *Journal of Sound and Vibration* 190 (2) (1996) 207–220.

[13] A.S. Ashour, Vibration of variable thickness plates with edges elastically restrained against translation and rotation, *Thin-Walled Structures* 42 (2004) 1–24.

[14] M. Amabili, A. Pasqualini, G. Dalpiaz, Natural frequencies and modes of free-edge circular plates vibrating in vacuum or in contact with liquid, *Journal of Sound and Vibration* 188 (5) (1995) 685–699.

[15] W.P. Rdzanek Jr., W.J. Rdzanek, Z. Engel, Theoretical analysis of sound radiation of an elastically supported circular plate, *Journal of Sound and Vibration* 265 (1) (2003) 155–174.

[16] K. Itao, S.H. Crandall, Natural modes and natural frequencies of uniform, circular, free-edge plates, *Journal of Applied Mechanics* 46 (1979) 448–453.

[17] Matlab® User's Guide, Mathworks, Inc., http://www.mathworks.com.